

Semiconductor-metal transition and magnetoresistance in $\text{La}_{(1+x)/3}\text{Ba}_{(2-x)/3}\text{Cu}_{1-x}\text{Mn}_x\text{O}_3$

S. L. Yuan

Department of Physics, Huazhong University of Science and Technology, Wuhan 430074, People's Republic of China

Y. Jiang and G. Li

Institute of Plasma Physics, Chinese Academy of Sciences, Hefei 230031, People's Republic of China

J. Q. Li

Department of Physics, Wuhan Automotive Polytechnic University, Wuhan 430070, People's Republic of China

Y. P. Yang and X. Y. Zeng

Department of Physics, Huazhong University of Science and Technology, Wuhan 430074, People's Republic of China

P. Tang and Z. Huang

Institute of Plasma Physics, Chinese Academy of Sciences, Hefei 230031, People's Republic of China

(Received 3 August 1999)

Samples of $\text{La}_{(1+x)/3}\text{Ba}_{(2-x)/3}\text{Cu}_{1-x}\text{Mn}_x\text{O}_3$ ($0.7 \leq x \leq 1$) were fabricated by solid-state reaction. X-ray diffraction reveals a structural distortion from the cubic perovskite to orthorhombic symmetry with increasing Cu doping content. The measurement of resistance vs temperature dependence in zero field shows a semiconductor-metal transition at T_p and a resistance minimum at low temperatures for the Cu doping range $\leq 20\%$. Applying a magnetic field of 5 T largely enhances the conductivity in the whole range of $T < T_p$ and the largest magnetoresistance effect appears around T_p . The double-exchange model is used to discuss the present observations in which the effects of A -site radius $\langle r_A \rangle$ and the A -site size mismatch σ^2 as well as the proportion of Mn^{4+} ions are considered. We also point out that the Cu ions enter into the Mn sites in the form of Cu^{3+} but not Cu^{2+} in order to explain the observed transition in samples with higher Cu doping contents.

In the past years, owing to the discovery of high-temperature superconductivity and colossal magnetoresistance (CMR), considerable attention was attracted to two types of transition-metal (Cu and Mn) oxides. Taking $\text{La}_{1+x}\text{Ba}_{2-x}\text{Cu}_3\text{O}_7$ and $\text{La}_{1+x}\text{Ba}_{2-x}\text{Mn}_3\text{O}_9$ as examples, it can be found that both systems have much in common. Among them, the most obvious fact is a mixed-valent behavior for transition-metal ions ($\text{Cu}^{2+}/\text{Cu}^{3+}$ and $\text{Mn}^{3+}/\text{Mn}^{4+}$) that strongly affect physical properties. Varying the relative ratio between La^{3+} and Ba^{2+} ions not only changes valence state of transition-metal, but also leads to some transformations of crystalline structure. With decreasing x , $\text{La}_{1+x}\text{Ba}_{2-x}\text{Cu}_3\text{O}_7$ undergoes a tetragonal-orthorhombic transition,¹ while $\text{La}_{1+x}\text{Ba}_{2-x}\text{Mn}_3\text{O}_9$ (or $\text{La}_{(1+x)/3}\text{Ba}_{(2-x)/3}\text{MnO}_3$) undergoes orthorhombic-rhombohedral-cubic-tetragonal/orthorhombic transitions.² The similarities between the two systems urges one to investigate the doping effect of Mn on Cu sites of $\text{La}_{1+x}\text{Ba}_{2-x}\text{Cu}_3\text{O}_7$ or of Cu on Mn sites of $\text{La}_{1+x}\text{Ba}_{2-x}\text{Mn}_3\text{O}_9$. Here we report effect of replacing Mn with Cu on the conducting properties of $\text{La}_{(1+x)/3}\text{Ba}_{(2-x)/3}\text{Cu}_{1-x}\text{Mn}_x\text{O}_3$. We find that even in the 20% Cu-doped sample both the semiconductor-metal transition and CMR effect are still observed. The experimental observations are discussed by considering effects of A -site ionic size ($\langle r_A \rangle$) and mismatch effect (σ^2) as well as the proportion of Mn^{4+} ions. Our analysis shows the main effect arising from the variation of the proportion of Mn^{4+} ions. We also point out that the Cu ions entering into the sample are Cu^{3+} but not Cu^{2+} ions.

A series of $\text{La}_{(1+x)/3}\text{Ba}_{(2-x)/3}\text{Cu}_{1-x}\text{Mn}_x\text{O}_3$ ($x=0.7, 0.8, 0.85, 0.9, 0.95, \text{ and } 1$) samples were prepared using the solid-state reaction method. Appropriate proportions of La_2O_3 , BaCO_3 , MnCO_3 and CuO high-purity powders were thoroughly mixed according to the desired stoichiometry, and then pre-fired at 1000°C for 24 h. The prepared powders were ground, pelletized, and sintered for three times at $1150^\circ\text{C}/24$ h, $1300^\circ\text{C}/72$ h, and $1250^\circ\text{C}/72$ h, respectively, with two intermediate careful grindings and mixing. After each sintering, the samples were cooled to room temperature at a rate of $40^\circ\text{C}/\text{h}$. X-ray powder diffraction shows that the thus prepared samples are single phase with no detectable secondary phases. Shown in Fig. 1 are powder x-ray-

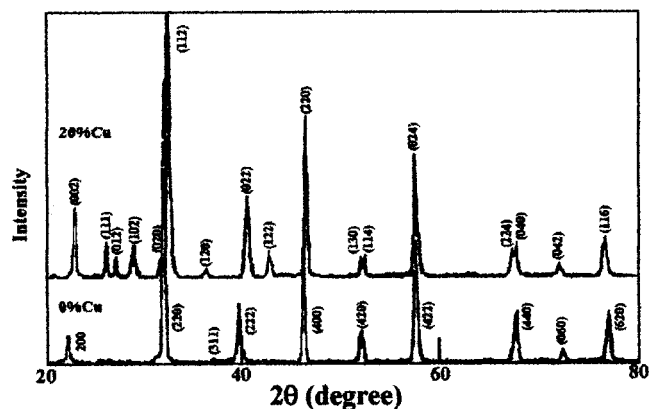


FIG. 1. X-ray powder-diffraction patterns for the Cu-free and 20% Cu-doped samples.

diffraction patterns obtained in the Cu-free and 20% Cu-doped samples. All diffraction peaks can be indexed to a cubic perovskite structure with $a \approx 7.811 \text{ \AA}$ for the Cu-free sample and an orthorhombic structure with $a = 7.683/\sqrt{2} \text{ \AA}$, $b = 7.862/\sqrt{2} \text{ \AA}$, and $c = 7.787 \text{ \AA}$ for the 20% Cu-doped sample. It implies that a structural distortion from the cubic perovskite to orthorhombic symmetry occurs with increasing the Cu doping content.

Resistance as a function of temperature was measured by the standard four-probe method. Figure 2 shows the experimental data obtained in zero magnetic field for samples of Cu doping content ranging between 0 and 20%, where the data are normalized by room-temperature resistance. As generally reported in the literature, the electrical conductivity of the Cu-free sample shows activated semiconducting behavior at high temperatures, and a transition to metallic behavior at low temperatures. The transition is characterized by a peak in the R vs T curve at the temperature T_p . Similar transition is also observed in the Cu-doped samples of $x \geq 0.8$, however, the conductivity at low temperatures does not exhibit metallic behavior. After passing through a minimum, further cooling brings about an increase in resistance. We point out that the observed minimum is an intrinsic behavior, but not due to the interplay between the conductivities of several phases because of no detectable secondary phases even in the 20% Cu-doped sample, as indicated by x-ray diffraction.

In Fig. 3(a), we plot the temperature T_p , corresponding to the peak in the R vs T curve, as a function of the Cu doping content. It can be found that T_p largely decreases when the Cu doping content increases from $\sim 5\%$ to $\sim 10\%$, and then tends to smoothly decrease on further increasing the Cu doping content. A large decrease in T_p with increasing the Cu doping content from $\sim 5\%$ to $\sim 10\%$ is consistent with a structural distortion from the cubic perovskite to orthorhombic symmetry.

We have also performed the measurement of R vs T dependence in a magnetic field of 5 T for the samples of Cu doping content ranging between 0 and 20%. The applied field enhances conductance near T_p for all the samples investigated, leading to an observation of the CMR effect. As an example, Fig. 4 shows the R - T data measured in the field for the 20% Cu-doped sample together with the corresponding zero-field data. As is evident in the figure, the magnetoresistance effect increases, reaches a maximum near T_p ,

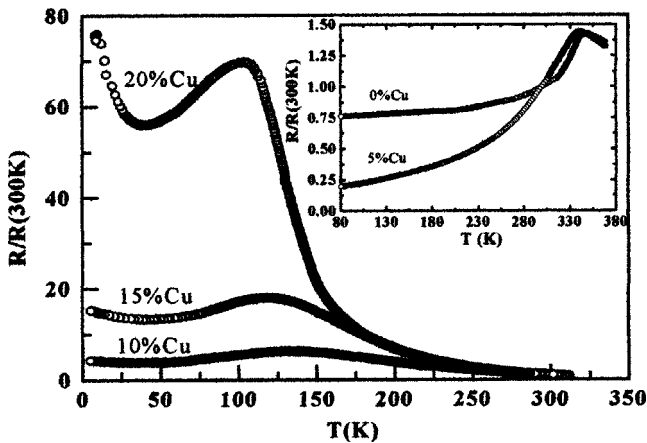


FIG. 2. Temperature dependence of resistance measured in zero field for $\text{La}_{(1+x)/3}\text{Ba}_{(2-x)/3}\text{Cu}_{(1-x)}\text{Mn}_x\text{O}_3$ samples.

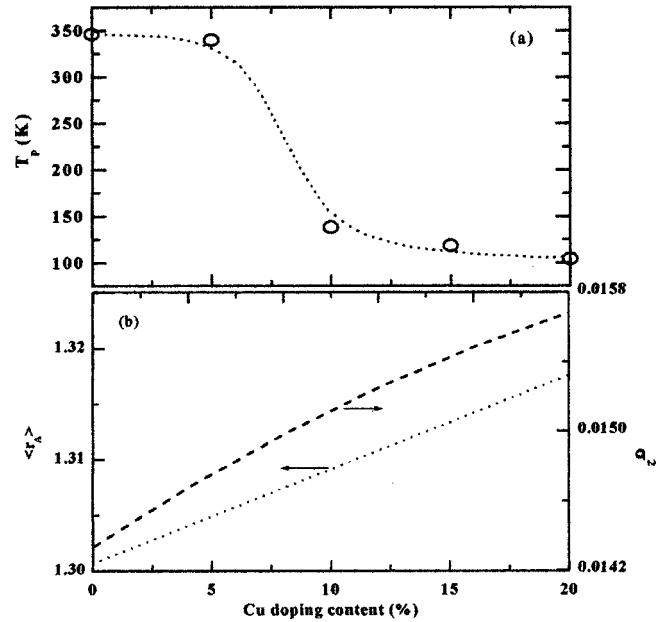


FIG. 3. (a) Transition temperature T_p determined by measuring zero-field R - T dependence and (b) the average A -site ionic size $\langle r_A \rangle$ as well as the A -site mismatch effect σ^2 as functions of the Cu doping content for $\text{La}_{(1+x)/3}\text{Ba}_{(2-x)/3}\text{Cu}_{(1-x)}\text{Mn}_x\text{O}_3$ samples.

and then decreases, as the sample is cooled. We also note that the magnetoresistance effect is significantly observed even at temperatures much lower than T_p , a behavior different from the previous observation in $\text{La}_{2/3}\text{B}_{1/3}\text{MnO}_3$ ($B = \text{Ca, Sr, Ba, Pb}$) in which no significant effect is observed at $T \ll T_p$.

Both magnetic and electronic properties in CMR materials have traditionally been understood by the double-exchange (DE) model.³ Although recent theoretical considerations⁴ indicated that the DE model alone could not quantitatively account for the observed CMR values, the model is still a good physical basis for the discussion of the fascinating properties of the CMR materials. The parent compound LaMnO_3 is an antiferromagnetic (AFM) insulator in which only Mn^{3+} exists. Doping with the divalent ions (Ca, Ba, etc.) causes the conversion of a proportional number of Mn^{3+} and Mn^{4+} . Because of the strong Hund's coupling,

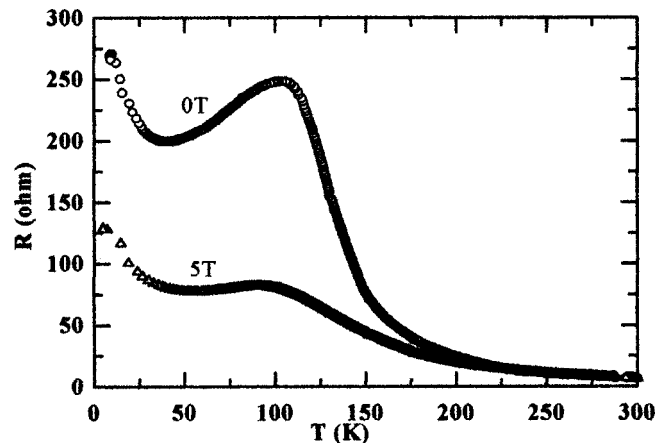
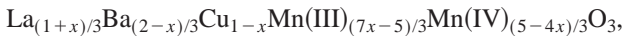


FIG. 4. Resistance vs temperature dependence measured in magnetic fields of $H = 0$ and 5 T in the 20% Cu-doped sample.

the electronic configurations are Mn^{3+} ($t_{2g}^3 e_g^1$) and Mn^{4+} ($t_{2g}^3 e_g^0$). A DE interaction between Mn^{3+} and Mn^{4+} mediates the ferromagnetic (FM) interaction, and the sample shows metallic conduction below a temperature T_p which is shown to be close to the Curie temperature T_c . Near T_p , the applied magnetic field tends to align the local t_{2g} spins, and then electron transfer increases. As a result, applying the field largely enhances the conductance, leading to the so-called CMR effect.

It is generally demonstrated that a stronger DE always corresponds to a higher transition temperature T_p . To date, the following three factors have been shown to strongly affect the DE (and hence T_p),⁵ i.e., the hole carriers density controlled by the $\text{Mn}^{3+}/\text{Mn}^{4+}$ ratio, the A-site cation size $\langle r_A \rangle$, and the A-site mismatch effect σ^2 defined by $\sigma^2 = \sum y_i r_i^2 - \langle r_A \rangle^2$. From the point view of being favorable to stabilize the low-temperature FM metallic phase one would expect an optimum $\text{Mn}^{3+}/\text{Mn}^{4+}$ ratio to be 2:1. On the other hand, the optimum $\text{Mn}^{3+}/\text{Mn}^{4+}$ ratio is favorable to form an ideal cubic perovskite. Any deviation from the ideal cubic perovskite would lead to a reduction in the Mn-O-Mn bond angle from 180° , which directly weakens the DE. Besides the $\text{Mn}^{3+}/\text{Mn}^{4+}$ ratio, both $\langle r_A \rangle$ and σ^2 have also been shown to influence the DE. Increasing $\langle r_A \rangle$ would strengthen the DE mainly due to the broadening of the one-electron e_g band, while the mismatch effect would promote the localization of e_g electrons thereby weakening the DE. For $\text{La}_{(1+x)/3}\text{Ba}_{(2-x)/3}\text{Mn}_x\text{Cu}_{1-x}\text{O}_3$, the stoichiometrical compositions for all metallic ions are varied with the Cu doping; as a result, variations in $\langle r_A \rangle$, σ^2 , and the $\text{Mn}^{3+}/\text{Mn}^{4+}$ ratio happen simultaneously. Shown in Fig. 3(b) are $\langle r_A \rangle$ and σ^2 as functions of the Cu doping content. It can be seen that both $\langle r_A \rangle$ and σ^2 increase with increasing the Cu doping content. Because of the almost same variation behavior in both $\langle r_A \rangle$ and σ^2 , we expect that the two effects would be approximately compensated for each other. Therefore, the main effect on T_p for the present system arises from the variation of $\text{Mn}^{3+}/\text{Mn}^{4+}$ ratio caused by the doping.

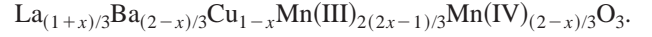
In the previous reports, Helmolt *et al.*⁶ observed semiconductor-metal transitions similar to the present observations except for different transition temperatures. They assumed the Cu ions existing in the system in the form of valence (2+). In this case, the composition of $\text{La}_{(1+x)/3}\text{Ba}_{(2-x)/3}\text{Cu}_{1-x}\text{Mn}_x\text{O}_3$ can be written as



where Mn(III) and Mn(IV) represent Mn^{3+} and Mn^{4+} ions, respectively. The proportion of Mn^{4+} ions is then simply calculated to be 33% ($x=1$), 42% ($x=0.95$), 52% ($x=0.9$), 63% ($x=0.85$), and 75% ($x=0.8$), respectively. Clearly, the proportion of Mn^{4+} ions exceeds 50% for Cu doping content higher than 10%. In this case, because the population of the hopping electrons from Mn^{3+} ions is smaller than the number of available hopping sites from Mn^{4+} ions, e_g electrons cannot gain enough kinetic energy to overcome the AFM exchange energy of t_{2g} spins. As a result, the low-temperature regime should exhibit an AFM insulating behavior. This is generally confirmed in systems such as $\text{La}_{0.5}\text{Ca}_{0.5}\text{MnO}_3$ (50% Mn^{4+}) (Ref. 7) or $\text{La}_{0.35}\text{Ca}_{0.65}\text{MnO}_3$ (65% Mn^{4+}),⁸ etc. However, our experi-

ments show that the semiconductor-metal transition can be observed even in the 20% Cu-doped sample in which the proportion of Mn^{4+} ions is as high as 75%.

In order to explain the semiconductor-metal transitions observed in the case of higher Cu doping content, we account for the Cu ions existing in the system in the form of valence (3+). In such a case, the composition can be rewritten as



The corresponding proportion of Mn^{4+} ions existing in the system is 33% ($x=1$), 36% ($x=0.95$), 41% ($x=0.9$), 45% ($x=0.85$), and 50% ($x=0.8$), respectively. Such proportions of Mn^{4+} ions are consistent with the experimental observations shown in Fig. 2. For the range of proportion of Mn^{4+} ions near 33%, the system is simply characterized by a semiconductor-metal transition on cooling, as seen in the Cu-free and 5% Cu-doped samples. Further increasing the Cu doping content increases the proportion of Mn^{4+} ions thereby weakening the ferromagnetic DE interaction. Consequently, the AFM superexchange interaction between the neighboring Mn ions cannot be completely suppressed. As it is well known, the ferromagnetic DE interaction favors e_g electrons to transfer between neighboring Mn ions, leading to a transition to FM metallic behavior at $T < T_p$. On the other hand, the AFM superexchange interaction prevents e_g electrons to transfer between neighboring Mn ions, leading to an increase in resistance at low temperatures. Their competition yields a minimum in the R vs T curve, which is indeed observed in the higher Cu-doped samples.

The considerations mentioned above can also account for the observed magnetoresistance properties. Cu doping on Mn sites of $\text{La}_{(1+x)/3}\text{Ba}_{(2-x)/3}\text{Cu}_{1-x}\text{Mn}_x\text{O}_3$ weakens the ferromagnetic DE interaction, so that the AFM interaction cannot be completely suppressed. The AFM interaction becomes stronger with decreasing temperature. Applying the magnetic field further suppresses the AFM interaction and hence promotes e_g electrons to transfer between neighboring Mn ions. This is the reason why the magnetoresistance effect can be significantly observed even at $T \ll T_p$.

In summary, the effect of Cu doping on conducting properties of $\text{La}_{(1+x)/3}\text{Ba}_{(2-x)/3}\text{Cu}_{1-x}\text{Mn}_x\text{O}_3$ has been experimentally studied. The semiconductor-metal transition moves to the low-temperature region with increasing the Cu doping content and disappears when the doping content exceeds 20%. The magnetoresistance effect can be significantly observed even in the 20% Cu-doped sample. The experimental observations are discussed within the framework of the DE model by taking into account the effects of A-site radius $\langle r_A \rangle$ and A-site disorder σ^2 as well as the $\text{Mn}^{3+}/\text{Mn}^{4+}$ ratio. Our analysis demonstrates that the main effect arises from the variation of $\text{Mn}^{3+}/\text{Mn}^{4+}$ ratio caused by the Cu doping. At the same time, we also point out that the Cu ions enter into the Mn sites in the form of Cu^{3+} but not Cu^{2+} .

This work was supported by Trans-Century Training Programme Foundation for the Talents by the Ministry of Education.

- ¹E. Takayama-Muromachi *et al.*, Jpn. J. Appl. Phys., Part 2 **26**, L1546 (1987); C. Dong *et al.*, Phys. Rev. B **37**, 5182 (1988); J. M. Newsam *et al.*, Solid State Ionics **32/33**, 1064 (1989).
- ²J. B. Goodenough *et al.*, *Magnetic and Other Properties of Oxides and Related Compounds*, Landolt-Börnstein, New Series, Group III, Vol. 4, pt. a (Springer, Berlin, 1970).
- ³C. Zener, Phys. Rev. **82**, 403 (1951); P.-G. De Gennes, *ibid.* **118**, 141 (1960).
- ⁴A. J. Millis *et al.*, Phys. Rev. Lett. **74**, 5144 (1995); H. Roder *et al.*, *ibid.* **76**, 1356 (1996).
- ⁵Lide M. Rodriguez-Martinez and J. Paul Attfield, Phys. Rev. B **54**, R15 622 (1996), and references therein.
- ⁶R. Von Helmolt *et al.*, Solid State Commun. **82**, 693 (1992).
- ⁷G. Q. Gong *et al.* J. Appl. Phys. **79**, 4538 (1996).
- ⁸M. R. Ibarra *et al.*, Phys. Rev. B **56**, 8252 (1997).